



Non-fragile robust output feedback control of uncertain active suspension systems with stochastic network-induced delay

Jing Zhao · Yajuan Zhu · Pak Kin Wong ·
Wenfeng Li · Zhixin Yang · Panshuo Li ·
Chonghui Song

Received: 20 July 2022 / Accepted: 30 December 2022 / Published online: 8 February 2023
© The Author(s), under exclusive licence to Springer Nature B.V. 2023

Abstract The vehicle active suspension has attracted considerable attention owing to its great contributions to the vertical dynamics of vehicle. This paper investigates the non-fragile output feedback control problem of the uncertain vehicle active suspension with stochastic network-induced delay. Firstly, taking the variation of sprung and unsprung masses into consideration, an interval type-2 (IT-2) Takagi–Sugeno (T–S) fuzzy model is introduced to describe the nonlinear characteristics of active suspension systems (ASSs). Secondly, to ensure that the control strategy is practicable when some states are unmeasured, a novel output feedback method is proposed by employing a variable substitution approach. Meanwhile, in order to approximate the real physical conditions of the control system, the gain perturbations are taken into account.

Thirdly, with regard to the complexity of signal transmission delay in network control process, a more generalized lumped delay form is employed to represent the network-induced delay. Moreover, to describe the stochasticity of lumped delay, a Markovian process is introduced. Finally, both numerical simulations and experimental tests are carried out to examine the effectiveness and practicability of the proposed controller.

Keywords Active suspension · Non-fragile control · Output feedback · Interval type-2 fuzzy model · Parameter uncertainties · Stochastic delay

1 Introduction

As an essential part of the automotive chassis, the suspension systems are required to satisfy the significant demands of driving safety, handling stability and ride comfort. Generally speaking, suspension systems can be classified into passive suspensions, semi-active suspensions, and active suspensions [1–3]. It is worth mentioning that the active suspension has great advantages in terms of improving vehicle ride comfort and handling stability, because it can forwardly generate and adjust the required control force according to different driving conditions.

It should be pointed out that the vehicle system parameters constantly vary along with the change of the driving environment in practical applications. This inevitably causes the parameter uncertainties of the

J. Zhao · Y. Zhu
School of Mechanical Engineering and Automation,
Northeastern University, Shenyang 110819, China

J. Zhao · Y. Zhu
Foshan Graduate School of Innovation, Northeastern
University, Foshan 528311, China

P. K. Wong (✉) · W. Li · Z. Yang
Department of Electromechanical Engineering, University
of Macau, Macau, China
e-mail: fstpkw@um.edu.mo

P. Li
School of Automation, Guangdong University of
Technology, Guangzhou 510062, China

C. Song
College of Information Science and Engineering, Northeastern
University, Shenyang 110819, China

active suspension systems (ASSs) [4]. To effectively address the inherent uncertainties in ASSs, the interval type-2 (IT-2) fuzzy method has been proven as an excellent tool, owing to its prominent ability of capturing system uncertainties [5,6]. An active levitation control system based on an interval IT-2 model-based fuzzy logic controller was investigated in [7]. Meanwhile, the suspension system is nonlinear due to the varying configuration. To deal with nonlinear systems, the Takagi–Sugeno (T–S) fuzzy model has been confirmed as a well-grounded method. For instance, the authors in [8] applied the T–S fuzzy method to explain the electrohydraulic ASSs with consideration of uncertain sprung mass and the control input. However, it is still challenging to handle the nonlinearity and uncertainties of the ASSs by an IT-2 T–S fuzzy model.

Apart from the construction of the ASSs model, the design of control strategy is also significant to refine the performance of the active suspension. Therefore, in recent ten years, researchers have proposed many feasible active suspension control strategies, such as sliding model control [9–12], adaptive control [13–15], and H_∞ control [16,17]. The H_∞ control has been widely investigated by researchers due to its good robustness and anti-interference ability. In general, the H_∞ control can be divided into state feedback H_∞ control and the output feedback H_∞ control. Given that not all state vectors can be measured online, the state feedback controller is not feasible in actual suspension system. Compared with the state feedback controller, the structure of output feedback controller is simpler and easier to implement [18]. Furthermore, the traditional H_∞ control is based on the premise that the controller can be realized accurately. However, it should be noted that the controller will be affected by many uncertain factors in practice, such as the delay of the actuator and the aging of the corresponding equipment [19–21]. These uncertainties could cause fragility of the controller and further lead to the degradation of the closed-loop system performance. Hence, much effort was devoted to deal with the controller fragility issue for suspension control systems, such as safety assessment method [22], fault-tolerant [23] method, and non-fragile method [24]. Among them, the non-fragile methods that can resist interference have attracted scholars' attention.

With the wide application of network communication technology in the field of vehicles, unlike the traditional point-to-point connection, the signal transmis-

sion delay may be an inevitable phenomenon due to the shared and band-limited channels of vehicle-mounted network [25]. The delay may lead to system oscillation and divergence in the operation of the active suspension system [26,27]. Nevertheless, previous studies regard this time delay as a fixed value [28], or only confine the upper and lower limits of the time delay and set the lower limit as zero [29]. However, in fact, this network-induced delay is usually a random phenomenon. Since the data transmission in the process of network control always exists, its lower limit cannot be zero. Therefore, it is necessary to design a more practical representation method of the network-induced time delay.

Based on the above motivations, this paper proposes an IT-2 fuzzy H_∞ controller for the uncertain ASSs with stochastic network-induced delay. The major contributions of this research are listed as follows:

- (1) An IT-2 T–S fuzzy method is developed to construct the model of the suspension system with parameter uncertainties.
- (2) A variable substitution approach is employed to calculate the output feedback control gains to reduce the computational burden and ensure satisfactory system response.
- (3) A more generalized lumped delay form is adopted to present the stochasticity of the network-induced delay to improve system stability and control effectiveness.

The rest of this work is organized as follows: Sect. 2 establishes the uncertain active suspension model and formulates the control objective. Section 3 presents the non-fragile output feedback controller design method. Simulation and experimental results are illustrated in Sects. 4 and 5, respectively. Finally, Sect. 6 concludes this research.

Notation With regard to a matrix X , X^{-1} and X^T denote its inverse and transpose, respectively. $[X]_s$ denotes $X + X^T$. The n -dimensional Euclidean space is denoted by R_n . $diag\{\cdot\}$ denotes a block diagonal matrix.

2 Modeling and problem formulation

2.1 Quarter-car ASS model

Figure 1 shows a common quarter-car active suspension model, and all symbol definitions of vehicle parameters

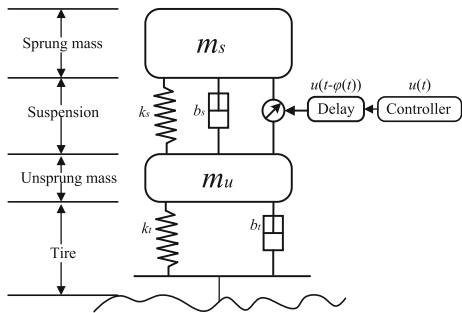


Fig. 1 Quarter-car automotive active suspension model

Table 1 Symbol definitions of vehicle model

Parameter	Physical meaning	Unit
$m_s(t)$	Sprung mass	kg
$m_u(t)$	Unsprung mass	kg
$z_s(t)$	Displacement of sprung mass	m
$z_u(t)$	Displacement of unsprung mass	m
$z_r(t)$	Displacement input of road	m
z_{max}	The maximum suspension travel limit	m
k_s	Stiffness of suspension	N/m
k_t	Stiffness of tire	N/m
b_s	Damping coefficient of suspension	N s/m
b_t	Damping coefficient of tire	N s/m
$u(t)$	Actuator force	N

are listed in Table 1. On the basis of the Newton’s second law, the vertical motion equations of suspension are acquired as:

$$\begin{cases} m_s \ddot{z}_s(t) = -b_s (\dot{z}_s(t) - \dot{z}_u(t)) - k_s (z_s(t) - z_u(t)) + u(t) \\ m_u \ddot{z}_u(t) = -b_t (\dot{z}_u(t) - \dot{z}_r(t)) - k_t (z_u(t) - z_r(t)) + b_s (\dot{z}_s(t) - \dot{z}_u(t)) + k_s (z_s(t) - z_u(t)) - u(t) \end{cases} \quad (1)$$

Define $x_1 = z_s(t) - z_u(t)$, $x_2 = \dot{z}_s(t)$, $x_3 = z_u(t) - z_r(t)$, $x_4 = \dot{z}_u(t)$.

The equations of vehicle suspension system in (1) can be presented as:

$$\dot{x}(t) = A(t)x(t) + B_\omega(t)\omega(t) + B_u(t)u(t) \quad (2)$$

where

$$x(t) = [x_1 \quad x_2 \quad x_3 \quad x_4]^T, \quad \omega(t) = \dot{z}_r(t),$$

$$A(t) = \begin{bmatrix} 0 & 1 & 0 & -1 \\ -\frac{k_s}{m_s(t)} & -\frac{b_s}{m_s(t)} & 0 & \frac{b_s}{m_s(t)} \\ 0 & 0 & 0 & 1 \\ \frac{k_s}{m_u(t)} & \frac{b_s}{m_u(t)} & -\frac{k_t}{m_u(t)} & -\frac{b_s+b_t}{m_u(t)} \end{bmatrix},$$

$$B_\omega(t) = \begin{bmatrix} 0 \\ 0 \\ -1 \\ \frac{b_t}{m_u(t)} \end{bmatrix}, \quad B_u(t) = \begin{bmatrix} 0 \\ \frac{1}{m_s(t)} \\ 0 \\ -\frac{1}{m_u(t)} \end{bmatrix}.$$

Considering that the aim of controller design is to enhance the ride comfort and guarantee the road holding ability, the controlled output can be expressed as:

$$\begin{cases} z_1(t) = \ddot{z}_s(t) \\ z_2(t) = \left[\frac{z_s(t) - z_u(t)}{z_{max}} \frac{k_t (z_u(t) - z_r(t))}{(m_s(t) + m_u(t)) g} \right]^T \end{cases}$$

As a result, (1) can be written as:

$$\begin{cases} \dot{x}(t) = A(t)x(t) + B_\omega(t)\omega(t) + B_u(t)u(t) \\ z_1(t) = C_1(t)x(t) + D_1(t)u(t) \\ z_2(t) = C_2(t)x(t) \end{cases} \quad (3)$$

$$C_1(t) = \begin{bmatrix} -\frac{k_s}{m_s(t)} & -\frac{b_s}{m_s(t)} & 0 & \frac{b_s}{m_s(t)} \end{bmatrix},$$

where $D_1(t) = \frac{1}{m_s(t)},$

$$C_2(t) = \begin{bmatrix} \frac{1}{z_{max}} & 0 & 0 & 0 \\ 0 & 0 & \frac{k_t}{(m_s(t)+m_u(t))g} & 0 \end{bmatrix}.$$

2.2 IT2-T-S model

With regard to uncertain variables $m_s(t)$ and $m_u(t)$, some assumptions are made as:

$$m_s(t) \in [m_{s \min}, m_{s \max}], \quad m_u(t) \in [m_{u \min}, m_{u \max}]$$

For brevity, the fuzzy membership functions are listed in Table 2, and the following definitions are given as:

$$\widehat{m}_s = \frac{1}{m_{s \max}} = \min \frac{1}{m_s(t)}, \quad \widehat{m}_u = \frac{1}{m_{u \max}} = \min \frac{1}{m_u(t)}$$

$$\widetilde{m}_s = \frac{1}{m_{s \min}} = \max \frac{1}{m_s(t)}, \quad \widetilde{m}_u = \frac{1}{m_{u \min}} = \max \frac{1}{m_u(t)}$$

Table 2 Fuzzy membership functions

Sprung mass	Unsprung mass
$\underline{\mu}_{M_{11}} = \underline{\mu}_{M_{21}} = \frac{\widetilde{m}_s - l_{11}}{\widetilde{m}_s - \widehat{m}_s}$	$\underline{\mu}_{M_{12}} = \underline{\mu}_{M_{22}} = \frac{\widetilde{m}_u - l_{21}}{\widetilde{m}_u - \widehat{m}_u}$
$\overline{\mu}_{M_{31}} = \overline{\mu}_{M_{41}} = \frac{l_{11} - \widehat{m}_s}{m_s - \widehat{m}_s}$	$\overline{\mu}_{M_{32}} = \overline{\mu}_{M_{42}} = \frac{l_{21} - \widehat{m}_u}{m_u - \widehat{m}_u}$
$\underline{\mu}_{M_{11}} = \underline{\mu}_{M_{21}} = \frac{\widetilde{m}_s - l_{12}}{\widetilde{m}_s - \widehat{m}_s}$	$\underline{\mu}_{M_{12}} = \underline{\mu}_{M_{22}} = \frac{\widetilde{m}_u - l_{22}}{\widetilde{m}_u - \widehat{m}_u}$
$\underline{\mu}_{M_{31}} = \underline{\mu}_{M_{41}} = \frac{l_{12} - \widehat{m}_s}{m_s - \widehat{m}_s}$	$\underline{\mu}_{M_{32}} = \underline{\mu}_{M_{42}} = \frac{l_{22} - \widehat{m}_u}{m_u - \widehat{m}_u}$

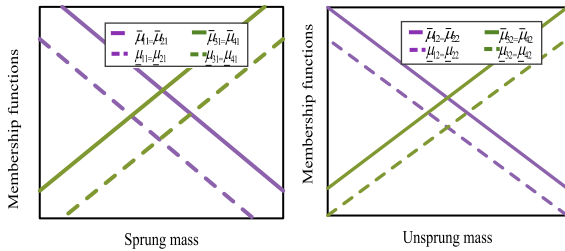


Fig. 2 Membership functions of the IT-2 fuzzy systems

$$l_{11}, l_{12} \in [\widehat{m}_s, \widetilde{m}_s], l_{11} = \frac{1}{m_s}, l_{12} < l_{11}$$

$$l_{21}, l_{22} \in [\widehat{m}_u, \widetilde{m}_u], l_{21} = \frac{1}{m_u}, l_{22} < l_{21}$$

These membership functions are plotted in Fig. 2.

Thereafter, the uncertain nonlinear suspension system is expressed by the following IT-2 T-S fuzzy models.

Model Rule *i*: If $\xi_1(t)$ is $M_{i1}(\xi_1(t))$, $\xi_2(t)$ is $M_{i2}(\xi_2(t))$, Then

$$\begin{cases} \dot{x}(t) = A_i x(t) + B_{\omega} \omega(t) + B_{ui} u(t) \\ z_1(t) = C_{1i} x(t) + D_{1i} u(t) \\ z_2(t) = C_{2i} x(t) \end{cases} \quad (4)$$

The interval set of the *i*th rule firing strength is as

$$\tilde{g}_i(\xi(t)) = \left[\underline{g}_i(\xi(t)), \overline{g}_i(\xi(t)) \right]$$

where $f = 1, 2, i = 1, 2, 3, 4$, $\xi(t)$ denotes the premise variables, $\underline{\mu}_{M_{if}}(\xi_f(t))$ and $\overline{\mu}_{M_{if}}(\xi_f(t))$ denote the lower membership function and upper membership function, $\underline{g}_i(\xi(t)) = \prod_{f=1}^4 \underline{\mu}_{M_{if}}(\xi_f(t))$ and $\overline{g}_i(\xi(t)) = \prod_{f=1}^4 \overline{\mu}_{M_{if}}(\xi_f(t))$ denote the lower grade of membership and upper grade of membership, and $0 \leq \underline{\mu}_{M_{if}}(\xi_f(t)) \leq \overline{\mu}_{M_{if}}(\xi_f(t))$, $\underline{g}_i(\xi(t)) \leq \overline{g}_i(\xi(t))$.

Then, the following definitions are given:

$$g_i(\xi(t)) = \underline{z}_i(\xi(t)) \underline{g}_i(\xi(t)) + \overline{z}_i(\xi(t)) \overline{g}_i(\xi(t))$$

$$\underline{z}_i(\xi(t)) + \overline{z}_i(\xi(t)) = 1$$

$$\sum_{i=1}^4 g_i(\xi(t)) = 1$$

Thus, the uncertain ASSs can be described as:

$$\begin{cases} \dot{x}(t) = \sum_{i=1}^4 g_i(\xi(t)) (A_i x(t) + B_{\omega i} \omega(t) + B_{ui} u(t)) \\ z_1(t) = \sum_{i=1}^4 g_i(\xi(t)) (C_{1i} x(t) + D_{1i} u(t)) \\ z_2(t) = \sum_{i=1}^4 g_i(\xi(t)) (C_{2i} x(t)) \end{cases} \quad (5)$$

where $A_i, B_{ui}, C_{1i}, D_{1i}, C_{2i}$ are obtained by replacing $\frac{1}{m_s(t)}$ and $\frac{1}{m_u(t)}$, with \widetilde{m}_s (or \widehat{m}_s) and \widetilde{m}_u (or \widehat{m}_u) in A, B_u, C_1, D_1, C_2 .

Then, for simplification, the system in (5) can be written as:

$$\begin{cases} \dot{x}(t) = A_s x(t) + B_{\omega s} \omega(t) + B_{us} u(t) \\ z_1(t) = C_{1s} x(t) + D_{1s} u(t) \\ z_2(t) = C_{2s} x(t) \end{cases} \quad (6)$$

where

$$A_s = \sum_{i=1}^4 g_i(\xi(t)) A_i, B_{\omega s} = \sum_{i=1}^4 g_i(\xi(t)) B_{\omega i},$$

$$B_{us} = \sum_{i=1}^4 g_i(\xi(t)) B_{ui}, C_{1s} = \sum_{i=1}^4 g_i(\xi(t)) C_{1i},$$

$$D_{1s} = \sum_{i=1}^4 g_i(\xi(t)) D_{1i}, C_{2s} = \sum_{i=1}^4 g_i(\xi(t)) C_{2i}.$$

Remark 1 It is worth noting that different from type-1 fuzzy method, the IT-2 fuzzy actual grades of membership $g_i(\xi(t))$ in (5) can be reconstructed as a linear combination of $\underline{g}_i(\xi(t))$ and $\overline{g}_i(\xi(t))$, characterized by the lower and upper membership functions $\underline{\mu}_{M_{is}}(\xi_s(t))$ and $\overline{\mu}_{M_{is}}(\xi_s(t))$, which are scaled by the nonlinear functions $\underline{z}_i(\xi(t))$ and $\overline{z}_i(\xi(t))$, respectively. This also means that IT-2 fuzzy sets consist of countless type 1 fuzzy sets. In other words, by using IT-2 fuzzy method, any membership function with uncertain parameters can be reconstructed by the upper and lower membership functions.

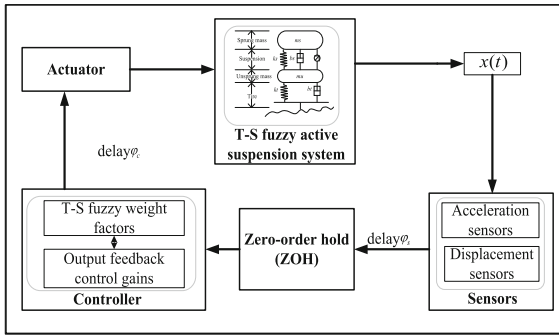


Fig. 3 Schematic diagram of the control-loop for the IT2 T-S fuzzy ASSs with stochastic network-induced delay

2.3 Non-fragile fuzzy controller with stochastic delay

Design of different membership functions for both the model and the controller is a challenging work without sufficient expert knowledge. However, with consideration of the model simplicity and controller effectiveness, fuzzy rules with the same membership functions are used for both the model and the controller. Figure 3 presents the schematic diagram of the control-loop for the IT2 T-S fuzzy ASSs with stochastic network-induced delay

Subsequently, a fuzzy controller is considered as follows:

Control Rule j : If $\xi_1(t)$ is $Mr(\xi_1(t))$, $\xi_2(t)$ is $Nr(\xi_2(t))$, Then

$$u(t) = \sum_{j=1}^4 \left(g_j^L(\xi(t)) + g_j^U(\xi(t)) \right) K_j x(t) \tag{7}$$

where

$$g_j^L \xi(t) = \frac{g_j(\xi(t))}{\sum_{j=1}^4 \left(\underline{g}_j(\xi(t)) + \bar{g}_j(\xi(t)) \right)},$$

$$g_j^U \xi(t) = \frac{\bar{g}_j(\xi(t))}{\sum_{j=1}^4 \left(\underline{g}_j(\xi(t)) + \bar{g}_j(\xi(t)) \right)}.$$

The perturbation of controller gain is represented by $\Delta K(t)$ and it is presumed to be a multiplication form as:

$$\Delta K(t) = HF(t)EK \tag{8}$$

where $F(t)$ is an unknown continuous function with time-varying characteristics; H and E are the preset real constant matrices.

Thus, the fuzzy control input can be rewritten as:

$$u(t) = \sum_{j=1}^4 g_j(\xi(t)) K_j (1 + HF(t)E)x(t) \tag{9}$$

where $g_j(\xi(t)) = \underline{g}_j(\xi(t)) + \bar{g}_j(\xi(t))$.

With the wide application of network communication technology in the field of vehicles, the signal transmission delay is a critical challenge. Due to the network-induced delay, the real controller can be depicted as:

$$u(t) = \sum_{j=1}^4 g_j(\xi(t)) K_j (1 + HF(t)E)x(t_k - \varphi_k),$$

$$0 < t_{k+1} - t_k, \triangleq h_k \leq h \tag{10}$$

where $t_k \leq t < t_{k+1}$, t_k denotes the k th sampling instant, h denotes the sampling period, the local control gain of j th fuzzy controller is expressed by K_j . The network-induced delay encountered at the sampling instant t_k is denoted as $\varphi_k = \varphi_s + \varphi_c$, where φ_s stands for the delay encountered in the sensor-to-controller link and φ_c stands for the delay encountered in the controller-to-actuator link. After defining $\varphi(t) = t - t_k - \varphi_k$, the controller in (10) can be depicted as:

$$u(t) = \sum_{j=1}^4 g_j(\xi(t)) K_j (1 + HF(t)E)x(t - \varphi_t) \tag{11}$$

In order to present a more generalized delay form, the randomness can be described as:

$$\text{prob}\{\varphi(t) \in [0, \varphi_l(t)]\} = \text{prob}\{\beta(t) = 1\} = \mathcal{E}\{\beta(t)\} = \beta$$

$$\text{prob}\{\varphi(t) \in [\varphi_l(t), \varphi_u(t)]\} = \text{prob}\{\beta(t) = 0\} = 1 - \mathcal{E}\{\beta(t)\} = 1 - \beta$$

where $0 < \varphi_l(t) < \varphi_u(t)$, $\beta(t)$ is a stochastic variable satisfying Bernoulli random, and $\mathcal{E}\{\beta(t)\}$ denotes the mathematical expectation of $\beta(t)$. Hence, the controller in (11) can be depicted as:

$$u(t) = \sum_{j=1}^4 g_j(\xi(t)) K_j (1 + HF(t)E) (\beta(t)x(t - \varphi_1(t)) + (1 - \beta(t))x(t - \varphi_2(t))) \tag{12}$$

where $\varphi_1(t)$ and $\varphi_2(t)$ are defined as :

$$\varphi_1(t) = \begin{cases} \varphi(t), & \varphi(t) \in [0, \varphi_l] \\ 0, & \varphi(t) \in (\varphi_l, \varphi_u] \end{cases}$$

$$\varphi_2(t) = \begin{cases} \varphi_l, & \varphi(t) \in [0, \varphi_l] \\ \varphi(t), & \varphi(t) \in (\varphi_l, \varphi_u] \end{cases}$$

Finally, by applying the non-fragile fuzzy controller in (15) to the fuzzy ASS in (5), the overall closed-loop system with parameter uncertainties and stochastic network-induced delay can be depicted as:

$$\begin{cases} \dot{x}(t) = f(t) + (\beta(t) - \beta)g(t) \\ z_1(t) = C_{1g}x(t) + \beta D_{1g}K_{sf}x(t - \varphi_1(t)) \\ \quad + (1 - \beta)D_{1g}K_{sf}x(t - \varphi_2(t)) \\ \quad + (\beta(t) - \beta)(D_{1g}K_{sf}x(t - \varphi_1(t))) \\ \quad - (\beta(t) - \beta)(D_{1g}K_{sf}x(t - \varphi_2(t))) \\ z_2(t) = C_{2g}x(t) \end{cases} \quad (13)$$

where

$$\begin{aligned} A_g &= \sum_{i=1}^4 g_i A_i, B_{\omega g} = \sum_{i=1}^4 g_i B_{\omega i}, B_{ug} \\ &= \sum_{i=1}^4 g_i \sum_{j=1}^4 g_j B_{ui}, \\ C_{1g} &= \sum_{i=1}^4 g_i C_{1i}, C_{2g} = \sum_{i=1}^4 g_i C_{2i}, D_{1g} \\ &= \sum_{i=1}^4 g_i \sum_{j=1}^4 g_j D_{1i}, \\ K_{sf} &= \sum_{j=1}^4 K_j(1 + HF(t)E), x(t) \\ &= \phi(t), t \in (-2\varphi_u, 0), \\ f(t) &= A_g x(t) + B_{\omega g} \omega(t) \\ &\quad + B_{ug} K_{sf} (\beta x(t - \varphi_1(t)) \\ &\quad \quad + (1 - \beta)x(t - \varphi_2(t))), \\ g(t) &= B_{ug} K_{sf} (x(t - \varphi_1(t)) - x(t - \varphi_2(t))). \end{aligned}$$

Briefly speaking, the objective of this work is to present a control strategy to compute a non-fragile fuzzy output feedback controller based on (12) for the IT2 T-S fuzzy ASSs. Then, the following conditions are satisfied:

- (1) The value of sprung mass acceleration needs to be minimal enough to improve ride comfort.
- (2) The closed-loop system in (13) is exponentially mean-square stable (EMSS) with the following γ attenuation level [30,31].
- (3) The mechanical constraints of the T-S fuzzy system in (13) are guaranteed [32]:

$$|\{z_2(t)\}_p| \leq 1, \quad p = 1, 2 \quad (14)$$

$$\left| \frac{u(t)}{u_{\max}} \right| \leq 1 \quad (15)$$

where $\{z_2(t)\}_p$ represents the p th row vector of $z_2(t)$, u_{\max} denotes the maximal actuator force.

After taking parameter uncertainties, controller fragile and stochastic delay into consideration, the closed-loop system in (13) is a stochastic system.

3 Main results

In this section, a novel non-fragile output feedback control algorithm is presented for uncertain ASSs with stochastic network-induced delay. This algorithm is efficient to ensure the stability and the expected performance indexes of the closed-loop system in (13).

3.1 Stability analysis

The following theorem proposed a set of sufficient conditions to guarantee that the closed-loop system in (13) is EMSS with γ attenuation level.

Theorem 1 *Considering the closed-loop system in (13), for given scalars $0 < \varphi_l < \varphi_u$, $\varphi_m = \varphi_u - \varphi_l$, $\beta \in [0, 1]$, $\delta^2 = \beta(1 - \beta)$ and γ , if there exist positive definite matrices $Q, P_1, P_2, Z_{11}, Z_{12}, Z_{21}, Z_{22}$, and general matrices M_1, M_2, M_3, M_4 , so that the following conditions hold, the closed-loop system in (13) is EMSS.*

$$\Xi_1 < 0, \Xi_2 < 0 \quad (16)$$

$$\Xi_3 < 0, \Xi_4 < 0 \quad (17)$$

$$\begin{bmatrix} -Q & \sqrt{\rho} \{C_{2i}\}_q^T \\ * & -I \end{bmatrix} < 0 \quad (18)$$

$$\begin{bmatrix} -I & \frac{\sqrt{\rho} K_{sf}}{u_{\max}} \\ * & -Q \end{bmatrix} < 0 \quad (19)$$

where

$$\begin{aligned} \Xi_1 &= \begin{bmatrix} \Phi & \sqrt{\varphi_l} [M_1, M_1] & \sqrt{\varphi_m} [M_3, M_3] \\ * & -Z_1 & 0 \\ * & * & -Z_2 \end{bmatrix}, \\ \Xi_2 &= \begin{bmatrix} \Phi & \sqrt{\varphi_l} [M_1, M_1] & \sqrt{\varphi_m} [M_4, M_4] \\ * & -Z_1 & 0 \\ * & * & -Z_2 \end{bmatrix}, \\ \Xi_3 &= \begin{bmatrix} \Phi & \sqrt{\varphi_l} [M_2, M_2] & \sqrt{\varphi_m} [M_3, M_3] \\ * & -Z_1 & 0 \\ * & * & -Z_2 \end{bmatrix}, \end{aligned}$$

$$\Xi_4 = \begin{bmatrix} \Phi & \sqrt{\varphi_l} [M_2, M_2] & \sqrt{\varphi_m} [M_4, M_4] \\ * & -Z_1 & 0 \\ * & * & -Z_2 \end{bmatrix},$$

$$\Phi = \Phi_1 + \Phi_2,$$

$$\Phi_1 = \text{diag} (P_1 + P_2, 0, -P_1, 0, -P_2, -\gamma^2 I) + 2 [N_1^T Q Y_f + M_1 N_2 + M_2 N_3 + M_3 N_4 + M_4 N_5],$$

$$\Phi_2 = [Y_f^T \quad \delta Y_g^T] [\varphi_l Z_1 + \varphi_m Z_2] [Y_f^T \quad \delta Y_g^T]^T + Z_{1m}^T Z_{1m} + Z_{2m}^T Z_{2m},$$

$$N_1 = [I \quad 0 \quad 0 \quad 0 \quad 0 \quad 0],$$

$$N_2 = [I \quad -I \quad 0 \quad 0 \quad 0 \quad 0],$$

$$N_3 = [0 \quad I \quad -I \quad 0 \quad 0 \quad 0],$$

$$N_4 = [0 \quad 0 \quad I \quad -I \quad 0 \quad 0],$$

$$N_5 = [0 \quad 0 \quad 0 \quad I \quad -I \quad 0],$$

$$Y_f = [A_g \quad B_{ug} K_{sf} \beta \quad 0 \quad B_{ug} K_{sf} (1 - \beta) \quad 0 \quad B_{\omega g}],$$

$$Y_g = [0 \quad B_{ug} K_{sf} \quad 0 \quad -B_{ug} K_{sf} \quad 0 \quad 0],$$

$$Z_{1m} = [C_{1g} \quad \beta D_{1g} K_{sf} \quad 0 \quad (1 - \beta) D_{1g} K_{sf} \quad 0 \quad 0],$$

$$Z_{2m} = [C_{2g} \quad 0 \quad 0 \quad 0 \quad 0 \quad 0],$$

$$Z_1 = \begin{bmatrix} Z_{11} & 0 \\ 0 & Z_{12} \end{bmatrix}, Z_2 = \begin{bmatrix} Z_{21} & 0 \\ 0 & Z_{22} \end{bmatrix}.$$

Proof A Lyapunov function $V(t)$ is chosen as follows:

$$\begin{aligned} V(t) &= x^T(t) Q x(t) + \int_{t-\varphi_l}^t x^T(\alpha) P_1 x(\alpha) d\alpha \\ &+ \int_{-\varphi_l}^0 \int_{t+a}^t [f^T(s), \delta g^T(s)] \\ &\times Z_1 [f^T(s), \delta g^T(s)]^T ds d\alpha \\ &+ \int_{-\varphi_u}^{-\varphi_l} \int_{t+a}^t [f^T(s), \delta g^T(s)] \\ &\times Z_2 [f^T(s), \delta g^T(s)]^T ds d\alpha \\ &+ \int_{t-\varphi_u}^t x^T(\alpha) P_2 x(\alpha) d\alpha \end{aligned} \tag{20}$$

Then, the derivative is obtained as follows:

$$\begin{aligned} \dot{V}(t) &= 2x^T(t) Q f(t) + x^T(t) P_1 x(t) + x^T(t) P_2 x(t) \\ &- x^T(t - \varphi_l) P_1 x(t - \varphi_l) \\ &- x^T(t - \varphi_u) P_2 x(t - \varphi_u) \\ &+ [f^T(t), \delta g^T(t)] \varphi_l Z_1 [f^T(t), \delta g^T(t)]^T \\ &- \int_{t-\varphi_l}^t [f^T(s), \delta g^T(s)] Z_1 [f^T(s), \delta g^T(s)]^T ds \\ &+ [f^T(t), \delta g^T(t)] \varphi_m Z_2 [f^T(t), \delta g^T(t)]^T \end{aligned}$$

$$- \int_{t-\varphi_u}^{t-\varphi_l} [f^T(s), \delta g^T(s)] Z_2 [f^T(s), \delta g^T(s)]^T ds \tag{21}$$

According to the basic theorem of calculus, the following equalities hold:

$$\begin{aligned} x(t) - x(t - \varphi_1(t)) - \int_{t-\varphi_1}^t f(s) \\ + g(s)(\beta(s) - \beta) ds &= 0 \\ x(t - \varphi_1(t)) - x(t - \varphi_l(t)) \\ - \int_{t-\varphi_l}^{t-\varphi_1(t)} f(s) + g(s)(\beta(s) - \beta) ds &= 0 \\ x(t - \varphi_l(t)) - x(t - \varphi_2(t)) \\ - \int_{t-\varphi_2(t)}^{t-\varphi_l} f(s) + g(s)(\beta(s) - \beta) ds &= 0 \\ x(t - \varphi_2(t)) - x(t - \varphi_u) \\ - \int_{t-\varphi_u}^{t-\varphi_2(t)} f(s) + g(s)(\beta(s) - \beta) ds &= 0 \end{aligned}$$

If the following equation is defined:

$$\xi^T(t) = [x^T(t), x^T(t - \varphi_1(t)), x^T(t - \varphi_l), x^T(t - \varphi_2(t)), x^T(t - \varphi_u), \omega^T(t)]$$

the following equations can hold:

$$\begin{aligned} 2\xi^T(t) M_1 [x(t) - x(t - \varphi_1(t)) \\ - \int_{t-\varphi_1(t)}^t f(s) + g(s)(\beta(s) - \beta) ds] &= 0 \\ 2\xi^T(t) M_2 [x(t - \varphi_1(t)) - x(t - \varphi_l(t)) \\ - \int_{t-\varphi_2(t)}^{t-\varphi_1(t)} f(s) + g(s)(\beta(s) - \beta) ds] &= 0 \\ 2\xi^T(t) M_3 [x(t - \varphi_l(t)) - x(t - \varphi_2(t)) \\ - \int_{t-\varphi_2(t)}^{t-\varphi_l} f(s) + g(s)(\beta(s) - \beta) ds] &= 0 \\ 2\xi^T(t) M_4 [x(t - \varphi_2(t)) - x(t - \varphi_u) \\ - \int_{t-\varphi_u}^{t-\varphi_2(t)} f(s) + g(s)(\beta(s) - \beta) ds] &= 0 \end{aligned}$$

Then, the following inequalities are obtained as:

$$\begin{aligned}
 & 2\xi^T(t)M_1[x(t) - x(t - \varphi_1(t)) \\
 & \quad - \int_{t-\varphi_1(t)}^t f(s) + g(s)(\beta(s) - \beta) ds] \\
 & \leq \varphi_1(t)\xi^T(t)[M_1, M_1]Z_1^{-1}[M_1, M_1]^T\xi(t) \\
 & \quad + \int_{t-\varphi_1(t)}^t [f^T(s), (\beta(s) - \beta)g^T(s)] \\
 & \quad \times Z_1[f^T(s), (\beta(s) - \beta)g^T(s)]^T ds \\
 & 2\xi^T(t)M_2[x(t - \varphi_1(t)) - x(t - \varphi_l(t)) \\
 & \quad - \int_{t-\varphi_l}^{t-\varphi_1(t)} f(s) + g(s)(\beta(s) - \beta) ds] \\
 & \leq (\varphi_l - \varphi_1(t))\xi^T(t)[M_2, M_2]Z_1^{-1}[M_2, M_2]^T \\
 & \xi(t) + \int_{t-\varphi_l}^{t-\varphi_1(t)} [f^T(s), (\beta(s) - \beta)g^T(s)] \\
 & Z_1[f^T(s), (\beta(s) - \beta)g^T(s)]^T ds \\
 & 2\xi^T(t)M_3[x(t - \varphi_l(t)) - x(t - \varphi_2(t)) \\
 & \quad - \int_{t-\varphi_2(t)}^{t-\varphi_l} f(s) + g(s)(\beta(s) - \beta) ds] \\
 & \leq (\varphi_2(t) - \varphi_l)\xi^T(t)[M_3, M_3]Z_2^{-1}[M_3, M_3]^T \\
 & \xi(t) + \int_{t-\varphi_l(t)}^{t-\varphi_2(t)} [f^T(s), (\beta(s) - \beta)g^T(s)] \\
 & Z_2[f^T(s), (\beta(s) - \beta)g^T(s)]^T ds \\
 & 2\xi^T(t)M_4[x(t - \varphi_2(t)) - x(t - \varphi_u)] \\
 & \quad - \int_{t-\varphi_u}^{t-\varphi_2(t)} f(s) + g(s)(\beta(s) - \beta) ds] \\
 & \leq (\varphi_u - \varphi_2(t))\xi^T(t)[M_4, M_4]Z_2^{-1}[M_4, M_4]^T \\
 & \xi(t) + \int_{t-\varphi_u}^{t-\varphi_2(t)} [f^T(s), (\beta(s) - \beta)g^T(s)] \\
 & Z_2[f^T(s), (\beta(s) - \beta)g^T(s)]^T ds \\
 & \text{By taking the expectation of } \dot{V}(t), \text{ it gives:} \\
 & \mathcal{E}V(t) \leq \mathcal{E} \left\{ \xi^T(t) \left[\hat{\Phi} + \varphi_1(t)[M_1, M_1]Z_1^{-1}[M_1, M_1]^T \right. \right. \\
 & \quad + (\varphi_l - \varphi_1(t))[M_2, M_2]Z_1^{-1}[M_2, M_2]^T \\
 & \quad + (\varphi_2(t) - \varphi_l)[M_3, M_3]Z_2^{-1}[M_3, M_3]^T \\
 & \quad \left. \left. + (\varphi_u - \varphi_2(t))[M_4, M_4]Z_2^{-1}[M_4, M_4]^T \right] \xi(t) \right\} \tag{22}
 \end{aligned}$$

Through applying Schur complement to (30), the following condition is true.

$$\varepsilon \left\{ z_1^T(t)z_1(t) - \gamma^2\omega^T(t)\omega(t) + \dot{V}(t) \right\} < 0 \tag{23}$$

According to Lemma 1 in [33], the closed-loop system in (13) is EMSS.

Under zero initial conditions, it can be obtained that $V(0) = 0, V(\infty) \geq 0$, and $\mathcal{E}\{\|z_1(t)\|_2\} < \gamma\mathcal{E}\{\|\omega(t)\|_2\}$ for all nonzero $\omega(t) \in L2[0, \infty]$. Hence, the closed-loop system in (13) satisfies the desired H_∞ robust requirement.

Based on (23), the following inequality is obtained:

$$\dot{V}(t) - \gamma^2w^T(t)w(t) < 0$$

Integrating two sides of the above inequality from zero to any $t > 0$, it can be acquired as:

$$V(t) - V(0) < \gamma^2 \int_0^t w^T(\tau)w(\tau)d\tau < \gamma^2\|w\|_2^2$$

Thus, the following inequality is obtained:

$$x^T(t)Qx(t) < \gamma^2\omega_{\max} + V(0)$$

Defining $\gamma^2\omega_{\max} + V(0) = \rho$, the following inequality holds as:

$$\begin{aligned}
 \max_{t>0} \left| \{z_2(t)\}_q \right|^2 & \leq \max_{t>0} \left\| \sum_{i=1}^4 h_i x^T(t)Q^{\frac{1}{2}} \right. \\
 Q^{-\frac{1}{2}} \{C_{2i}\}_q^T \{C_{2i}\}_q Q^{\frac{1}{2}} Q^{-\frac{1}{2}} x(t) \left. \right\|_2
 \end{aligned}$$

It leads to that the constraints in (14) are guaranteed, if

$$\rho \cdot \sum_{i=1}^4 h_i Q^{-\frac{1}{2}} \{C_{2i}\}_q^T \{C_{2i}\}_q Q^{-\frac{1}{2}} < I \tag{24}$$

Through applying Schur complement to (20), the following inequality is obtained as:

$$\frac{\rho x(t)K_{sf}K_{sf}^T x^T(t)}{u_{\max}^2} < x(t)Qx^T(t) < \rho$$

which means the constraints in (15) are guaranteed. Thus, the proof is completed.

3.2 The state feedback control design

Taking gain perturbations into account, the following theorem is obtained based on Theorem 1 to calculate the desired state feedback controller gains.

Theorem 2 *Considering the closed-loop system in (13), with regard to given scalars γ , $0 < \varphi_l < \varphi_u$, $\varphi_m = \varphi_u - \varphi_l$, $\beta \in [0, 1]$, $\delta^2 = \beta(1 - \beta)$, and $\Delta Kx(t) < \Delta u_{\max}$, the closed-loop system in (13) is EMSS, if there exist positive definite matrices $P, \bar{P}, \check{P}_1, \check{P}_2, \check{Z}_1, \check{Z}_2$, and general matrices $\check{M}_1, \check{M}_2, \check{M}_3, \check{M}_4$, such that the following conditions apply to $i, j = 1, 2, 3, 4$.*

$$\begin{bmatrix} \check{\Xi}_{1ij} & \Pi \\ * & \Lambda \end{bmatrix} < 0, \begin{bmatrix} \check{\Xi}_{2ij} & \Pi \\ * & \Lambda \end{bmatrix} < 0 \tag{25}$$

$$\begin{bmatrix} \check{\Xi}_{3ij} & \Pi \\ * & \Lambda \end{bmatrix} < 0, \begin{bmatrix} \check{\Xi}_{4ij} & \Pi \\ * & \Lambda \end{bmatrix} < 0 \tag{26}$$

$$\begin{bmatrix} -I & \sqrt{\rho} \{C_{2i}\}_q P \\ * & -P \end{bmatrix} < 0 \tag{27}$$

$$\begin{bmatrix} -I & \frac{\sqrt{\rho} V_j}{u_{\max} - \Delta u_{\max}} \\ * & -P \end{bmatrix} < 0 \tag{28}$$

Moreover, the state feedback controller gains are achieved as:

$$K_{sf}^i = V_j P^{-1}$$

where

$$\check{\Xi}_{1ij} = \begin{bmatrix} \check{\Phi} & \sqrt{\varphi_l} [\check{M}_1, \check{M}_1] & \sqrt{\varphi_m} [\check{M}_3, \check{M}_3] & \check{\Gamma}_1 \\ * & \check{Z}_1 - 2\check{P} & 0 & 0 \\ * & * & \check{Z}_1 - 2\check{P} & 0 \\ * & * & * & \check{\Gamma}_2 \end{bmatrix},$$

$$\check{\Xi}_{2ij} = \begin{bmatrix} \check{\Phi} & \sqrt{\varphi_l} [\check{M}_1, \check{M}_1] & \sqrt{\varphi_m} [\check{M}_4, \check{M}_4] & \check{\Gamma}_1 \\ * & \check{Z}_1 - 2\check{P} & 0 & 0 \\ * & * & \check{Z}_1 - 2\check{P} & 0 \\ * & * & * & \check{\Gamma}_2 \end{bmatrix},$$

$$\check{\Xi}_{3ij} = \begin{bmatrix} \check{\Phi} & \sqrt{\varphi_l} [\check{M}_2, \check{M}_2] & \sqrt{\varphi_m} [\check{M}_3, \check{M}_3] & \check{\Gamma}_1 \\ * & \check{Z}_1 - 2\check{P} & 0 & 0 \\ * & * & \check{Z}_1 - 2\check{P} & 0 \\ * & * & * & \check{\Gamma}_2 \end{bmatrix},$$

$$\check{\Xi}_{4ij} = \begin{bmatrix} \check{\Phi} & \sqrt{\varphi_l} [\check{M}_2, \check{M}_2] & \sqrt{\varphi_m} [\check{M}_4, \check{M}_4] & \check{\Gamma}_1 \\ * & \check{Z}_1 - 2\check{P} & 0 & 0 \\ * & * & \check{Z}_1 - 2\check{P} & 0 \\ * & * & * & \check{\Gamma}_2 \end{bmatrix}$$

$$\Pi = [\Pi_1 \quad \Pi_2],$$

$$\Pi_1 = \begin{bmatrix} \varepsilon_1 B_{ug} H F & 0 \\ 0 & 0 \\ 0 & 0 \\ \varepsilon_1 \sqrt{\varphi_l} B_{ug} H F & 0 \\ 0 & \varepsilon_2 \sqrt{\varphi} \delta B_{ug} H F \\ \varepsilon_1 \sqrt{\varphi_l} B_{ug} H F & 0 \\ 0 & \varepsilon_2 \sqrt{\varphi_m} \delta B_{ug} H F \\ \varepsilon_1 D_{li} H F & 0 \end{bmatrix},$$

$$\Pi_2 = \begin{bmatrix} 0 & 0 \\ \beta (EV_j)^T & (EV_j)^T \\ 0 & 0 \\ (1 - \beta) (EV_j)^T & -(EV_j)^T \\ 0 & 0 \\ 0 & 0 \\ 0 & 0 \\ 0 & 0 \end{bmatrix},$$

$$\Lambda = \text{diag} (-\varepsilon_1 I, -\varepsilon_2 I, -\varepsilon_1 I, -\varepsilon_2 I, -\varepsilon_1 I, -\varepsilon_2 I),$$

$$\check{\Phi} = \text{diag} (\check{P}_1 + \check{P}_2, 0, -\check{P}_1, 0, -\check{P}_2, -\gamma^2 I),$$

$$+ \text{sym} [N_1^T \check{Y}_f + \check{M}_1 N_2 + \check{M}_2 N_3 + \check{M}_3 N_4 + \check{M}_4 N_5],$$

$$\check{\Gamma}_2 = \text{diag} (-\check{Z}_{11} \quad -\check{Z}_{12} \quad -\check{Z}_{21} - \check{Z}_{22} \quad -I \quad -I),$$

$$\check{Y}_f = [A_i P \quad B_{ui} V_j \beta \quad 0 \quad B_{ui} V_j (1 - \beta) \quad 0 \quad B_{\omega i}]$$

$$\check{Y}_g = [0 \quad B_{ui} V_j \quad 0 \quad -B_{ui} V_j \quad 0 \quad 0],$$

$$\check{Z}_{1m} = [C_{1i} P \quad \beta D_{1i} V_j \quad 0 \quad (1 - \beta) D_{1i} V_j \quad 0 \quad 0],$$

$$\check{Z}_{2m} = [C_{2i} P \quad 0 \quad 0 \quad 0 \quad 0 \quad 0],$$

$$\check{Z}_1 = \begin{bmatrix} \check{Z}_{11} & 0 \\ 0 & \check{Z}_{12} \end{bmatrix}, \check{P} = \begin{bmatrix} P & 0 \\ 0 & P \end{bmatrix},$$

$$\check{Z}_2 = \begin{bmatrix} \check{Z}_{21} & 0 \\ 0 & \check{Z}_{22} \end{bmatrix}.$$

Proof The following conditions are defined as:

$$\check{Z}_1 = Z_1^{-1}, \check{Z}_2 = Z_2^{-1}$$

$$P = Q^{-1}, V = K_{sf} P, \bar{P} = P^T Q P$$

$$\check{M}_1 = P M_1 P, \check{M}_2 = P M_2 P$$

$$\check{M}_3 = P M_3 P, \check{M}_4 = P M_4 P$$

$$\Theta = \text{diag} (P_n I P P P P I_s), n = 6, s = 8.$$

After replacing the corresponding matrix in (25) and (26), followed by pre-multiplying and post-multiplying (25) and (26) by diagonal matrix Θ . (16) and (17) are then obtained by replacing $\check{Z}_k - 2\check{P}$ to $-\check{P} \check{Z}_k^{-1} \check{P}$, where $k = 1, 2$. Thus, Theorem 2 is obtained.

Remark 2 $\Delta Kx(t) < \Delta u_{\max}$ is the bound of gain perturbations $\Delta K(t)$. Considering the fragility of the controller, the gain perturbation $\Delta K(t)$ is introduced into Theorems 2–3 to improve the anti-interaction ability of the suspension controller, but the gain perturbations are not infinite. Referring to [34], the bound is assumed as $\Delta Kx(t) < \Delta u_{\max}$.

3.3 The output feedback control design

The measured output vector is defined as follows:

$$y(t) = Cx(t) \tag{29}$$

where

$$C = \begin{bmatrix} 1 & 0 & 0 & 0 \\ 0 & 1 & 0 & 0 \\ 0 & 0 & 0 & 1 \end{bmatrix}.$$

According to the relationship between state feedback and output feedback, the following equality holds [35]:

$$K_{sf} = K_{sof}C = VP^{-1} \tag{30}$$

The following equations are also defined as:

$$P = SP_N S^T + RP_R R^T$$

$$V = V_R R^T$$

$$R = C^\dagger + SL$$

where K_{sf} denotes the feedback control gains, K_{sof} denotes the output feedback control gain, P_N, P_R are positive definite matrices, S is the null space of C , L is an arbitrary matrix.

Based on (25)–(30), a non-fragile output feedback controller is presented in the following theorem.

Theorem 3 *Considering the closed-loop system in (13), for given scalars $\gamma, 0 < \varphi_l < \varphi_u, \varphi_m = \varphi_u - \varphi_l, \beta \in [0, 1], \delta^2 = \beta(1 - \beta)$ and $\Delta Kx(t) < \Delta u_{max}$, the closed-loop system in (13) is EMSS, if there exist positive definite matrices $\bar{Q}, \bar{P}_1, \bar{P}_2, \bar{Z}_1, \bar{Z}_2$, and general matrices $\bar{M}_1, \bar{M}_2, \bar{M}_3, \bar{M}_4$, such that the following conditions hold true for $i, j = 1, 2, 3, 4$.*

$$\begin{bmatrix} \bar{E}_{1ij} & \bar{\Pi} \\ * & \Lambda \end{bmatrix} < 0, \quad \begin{bmatrix} \bar{\Xi}_{2ij} & \bar{\Pi} \\ * & \Lambda \end{bmatrix} < 0 \tag{31}$$

$$\begin{bmatrix} \bar{\Xi}_{3ij} & \bar{\Pi} \\ * & \Lambda \end{bmatrix} < 0, \quad \begin{bmatrix} \bar{\Xi}_{4ij} & \bar{\Pi} \\ * & \Lambda \end{bmatrix} < 0 \tag{32}$$

$$\begin{bmatrix} -(SP_N S^T + RP_R R^T) & * \\ * & * \\ \sqrt{\rho}(SP_N S^T + RP_R R^T) \{C_{2i}\}_q^T & -I \end{bmatrix} < 0 \tag{33}$$

$$\begin{bmatrix} -I & \frac{\sqrt{\rho}RV_{Ri}^T}{u_{max} - \Delta u_{max}} \\ * & SP_N S^T + RP_R R^T \end{bmatrix} < 0 \tag{34}$$

Moreover, the output feedback controller gains are obtained as:

$$K_{sof}^i = V_{Rj} P_R^{-1}$$

where

$$\bar{\Xi}_{1ij} = \begin{bmatrix} \bar{\Phi} & \sqrt{\varphi_l} [\bar{M}_1, \bar{M}_1] & \sqrt{\varphi_m} [\bar{M}_3, \bar{M}_3] & \bar{\Gamma}_1 \\ * & \bar{Z}_1 - 2\bar{P} & 0 & 0 \\ * & * & \bar{Z}_2 - 2\bar{P} & 0 \\ * & * & * & \bar{\Gamma}_2 \end{bmatrix},$$

$$\bar{\Xi}_{2ij} = \begin{bmatrix} \bar{\Phi} & \sqrt{\varphi_i} [\bar{M}_1, \bar{M}_1] & \sqrt{\varphi_m} [\bar{M}_4, \bar{M}_4] & \bar{\Gamma}_1 \\ * & \bar{Z}_1 - 2\bar{P} & 0 & 0 \\ * & * & \bar{Z}_2 - 2\bar{P} & 0 \\ * & * & * & \bar{\Gamma}_2 \end{bmatrix},$$

$$\bar{\Xi}_{3ij} = \begin{bmatrix} \bar{\Phi} & \sqrt{\varphi_l} [\bar{M}_2, \bar{M}_2] & \sqrt{\varphi_m} [\bar{M}_3, \bar{M}_3] & \bar{\Gamma}_1 \\ * & \bar{Z}_1 - 2\bar{P} & 0 & 0 \\ * & * & \bar{Z}_2 - 2\bar{P} & 0 \\ * & * & * & \bar{\Gamma}_2 \end{bmatrix},$$

$$\bar{\Xi}_{4ij} = \begin{bmatrix} \bar{\Phi} & \sqrt{\varphi_l} [\bar{M}_2, \bar{M}_2] & \sqrt{\varphi_m} [\bar{M}_4, \bar{M}_4] & \bar{\Gamma}_1 \\ * & \bar{Z}_1 - 2\bar{P} & 0 & 0 \\ * & * & \bar{Z}_2 - 2\bar{P} & 0 \\ * & * & * & \bar{\Gamma}_2 \end{bmatrix},$$

$$\bar{\Pi} = [\bar{\Pi}_1 \quad \bar{\Pi}_2],$$

$$\bar{\Pi}_1 = \begin{bmatrix} \varepsilon_1 B_{ug} H F & 0 \\ 0 & 0 \\ 0 & 0 \\ \varepsilon_1 \sqrt{\varphi_l} B_{ug} H F & 0 \\ 0 & \varepsilon_2 \sqrt{\varphi} \delta B_{ug} H F \\ \varepsilon_1 \sqrt{\varphi_l} B_{ug} H F & 0 \\ 0 & \varepsilon_2 \sqrt{\varphi_m} \delta B_{ug} H F \\ \varepsilon_1 D_{li} H F & 0 \end{bmatrix},$$

$$\bar{\Pi}_2 = \begin{bmatrix} 0 & 0 \\ \beta (E V_{Rj} R^T)^T & (E V_{Rj} R^T)^T \\ 0 & 0 \\ (1 - \beta) (E V_{Rj} R^T)^T & - (E V_{Rj} R^T)^T \\ 0 & 0 \\ 0 & 0 \\ 0 & 0 \\ 0 & 0 \end{bmatrix},$$

$$\bar{\Phi} = \text{diag} (\bar{P}_1 + \bar{P}_2, 0, -\bar{P}_1, 0, -\bar{P}_1, -\gamma^2 I),$$

$$+ \text{sym} [N_1^T \bar{Y}_f + \bar{M}_1 N_2 + \bar{M}_2 N_3 + \bar{M}_3 N_4 + \bar{M}_4 N_5],$$

$$\bar{\Gamma}_2 = \text{diag} (-\bar{Z}_{11} - \bar{Z}_{12} - \bar{Z}_{21} - \bar{Z}_{22} \quad -I - I),$$

$$\bar{Y}_f = \begin{bmatrix} A_i (SP_N S^T + RP_R R^T) & B_{1i} V_{Rj} R^T \beta & 0 \\ B_{ui} V_{Rj} R^T (1 - \beta) & 0 & B_{\omega} \end{bmatrix},$$

$$\bar{Y}_g = [0 \quad B_{ui} V_{Rj} R^T \quad 0 \quad -B_{ui} V_{Rj} R^T \quad 0 \quad 0],$$

$$\bar{Z}_{2m} = [C_{2i} (SP_N S^T + RP_R R^T) \quad 0 \quad 0 \quad 0 \quad 0 \quad 0],$$

$$\bar{Z}_1 = \begin{bmatrix} \bar{Z}_{11} & 0 \\ 0 & \bar{Z}_{12} \end{bmatrix}, \bar{Z}_2 = \begin{bmatrix} \bar{Z}_{21} & 0 \\ 0 & \bar{Z}_{22} \end{bmatrix},$$

$$\bar{P} = \begin{bmatrix} SP_N S^T + RP_R R^T & 0 \\ 0 & SP_N S^T + RP_R R^T \end{bmatrix}.$$

3.4 Algorithm

To find a better gain matrix with a more advantageous performance, the following Algorithm 1 is presented to further obtain a better solution based on the two-step method [4]. The two-step method can effectively calculate the optimal output feedback controller based on the state feedback controller without redundant iteration. Besides, the first step is to solve Theorem 2 to obtain the transitional arbitrary matrix L , and the second step is to solve Theorem 3 on the basis of first step to finally obtain the output feedback gain directly.

Algorithm 1

Step 1: Input scalars $\varphi_l, \rho, \varphi_u, \varphi_m, \beta$ and δ and solve the Linear matrix inequality (LMI) optimization problem Q_s .

$$Q_s : \begin{cases} \text{minimize } \gamma \\ \text{s.t. } P > 0, V > 0, \check{P}_1 > 0, \check{P}_2 > 0, \check{Z}_1 > 0 \\ \check{Z}_2 > 0, \Delta K < \Delta u_{\max}, \text{ LMIs (25) -- (28)} \end{cases}$$

Step 2: If Q_s is feasible, Matrix L can be defined as: $L = S^\dagger P C^T (C P C^T)^{-1}$

Step 3: Solve the LMI optimization problem Q_o , the output feedback control gain can be obtained as $K_{sof}^i = V_{Rj} P_R^{-1}$.

$$Q_o : \begin{cases} \text{minimize } \gamma \\ \text{s.t. } P_R > 0, V_R > 0, \bar{P}_1 > 0, \bar{P}_2 > 0, \bar{Z}_1 > 0 \\ \bar{Z}_2 > 0, \Delta K < \Delta u_{\max} \text{ LMIs (31) -- (34)} \end{cases}$$

Remark 3 It is noteworthy that the value of Matrix S also has a great influence on K_{sof} , and its value should be adjusted appropriately in the process of solving. If the performance of the optimized control gain matrix K_{sof} is better than before, then the procedure is stopped.

4 Simulation results

In this section, some numerical simulations on a quarter-car ASS model are executed to estimate and verify the performance of the designed control algorithm. Table 3 lists the relevant parameters of the quarter-car ASS model.

In order to more highlight the effectiveness of the presented control method, the control methods in [16, 17, 34] introduced for comparison. Given that the authors in [34] presented a non-fragile controller without time delay, or the ease of expression, this set of the comparison is represented as Cases 1- 4 with different controller parameter perturbation as shown in

Table 3 Vehicle parameters and values

Parameter	Value	Unit	Parameter	Value
$m_s(t)$	[256,384]	kg	z_{\max}	0.1 m
$m_u(t)$	[35,45]	kg	Δu_{\max}	50 N
k_s	18000	N/m	u_{\max}	2500 N
k_t	200000	N/m	φ_l	0.035 s
b_s	1000	N s/m	φ_d	0.095 s
b_t	10	N s/m		

Table 4 Control perturbation cases in stimulation

Case number	H	F	E	ΔK
Case 1	0	0	0	0
Case 2	1	1	0.2	0.2K
Case 3	1	-1	0.3	-0.3K
Case 4	1	1	0.4	0.4K

Table 4. The aim of this comparison is to clarify the effectiveness with consideration of time delay in the ASSs. The authors in [16] presented an output feedback controller with time delay which is not stochastic. In order to highlight the effectiveness of the stochastic method, we compare the presented controller with the controller in [16], which is reflected as Case 1. The authors in [17] proposed a fuzzy controller without considering non-fragile. Thus, we compare the proposed controller with the controller in [17] to emphasize the importance of the non-fragile control.

Remark 4 It is known that the state feedback system requires the measurement of every component of the state. However, in practical applications, it is not always possible to access all state variables, and only partial information is available through measured outputs. Compared with the state feedback control system, the output feedback control system is a low-cost solution which does not require full information of the state variables. However, the difference of the control effect with the two control methods is not obvious and cannot be easily figured out in the simulation stage, so the comparisons are not conducted in this work.

With mincx solver in the LMI toolbox, the following local control gains and compared gains are obtained as:

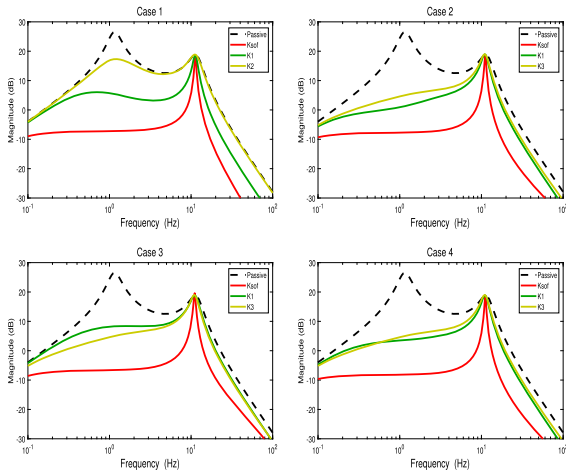


Fig. 4 Frequency responses of vehicle body acceleration in Case 1, Case 2, Case 3, and Case 4

Case 1 :

$$K = 10^4 \times [-1.2089 - 4.1497 - 0.0079]$$

$$K1 = 2500 \times [5.2122 - 0.6415 - 0.2503]$$

$$K2 = 10^4 \times [1.7417 \ 0.5445 \ 0.0399 - 0.0314]$$

Case 2:

$$K = 10^4 \times [-1.7650 - 5.5251 - 0.0185]$$

$$K1 = 2500 \times [4.4865 - 1.3724 - 0.1413]$$

$$K3 = 10^4 \times [1.6026 - 0.1181 - 0.2097 - 0.0333]$$

Case 3:

$$K = 10^4 \times [-1.6826 - 5.4481 - 0.0110]$$

$$K1 = 2500 \times [3.1293 - 2.4439 - 0.1658]$$

$$K3 = 10^4 \times [1.6026 - 0.1181 - 0.2097 - 0.0333]$$

Case 4:

$$K = 10^4 \times [-1.5368 - 5.0442 - 0.0015]$$

$$K1 = 2500 \times [2.4183 - 1.6881 - 0.1200]$$

$$K3 = 10^4 \times [1.6026 - 0.1181 - 0.2097 - 0.0333]$$

4.1 Frequency responses

The frequency response is used to show the interference attenuation performance in this section. The controller designed in this paper is K , which is represented by a red solid line. And the compared controller in [34] is $K1$, which is represented by a green dotted line. And the compared controllers in [16, 17] are

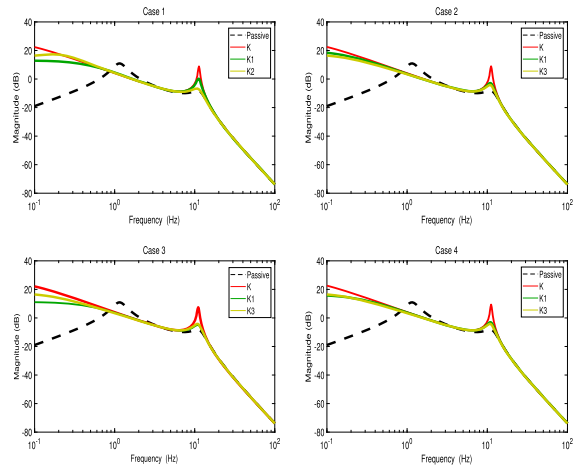


Fig. 5 Frequency responses of relative suspension travel in Case 1, Case 2, Case 3, and Case 4

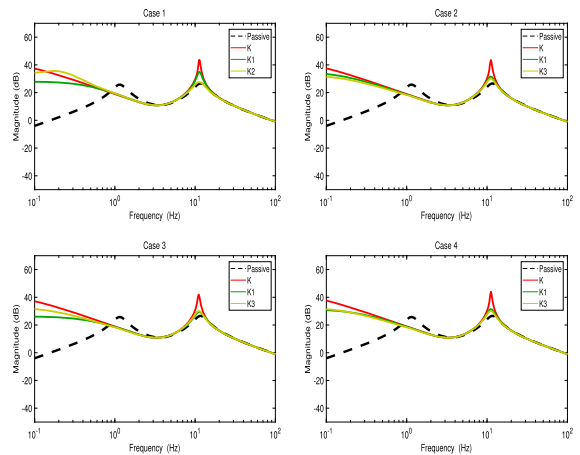


Fig. 6 Frequency responses of suspension relative dynamic load in Case 1, Case 2, Case 3, and Case 4

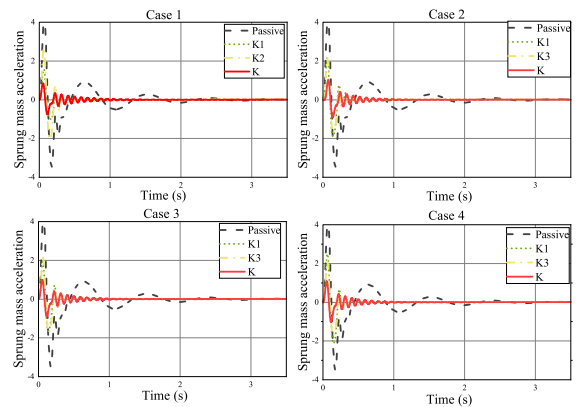


Fig. 7 Sprung mass acceleration under bump excitation in Case 1, Case 2, Case 3, and Case 4

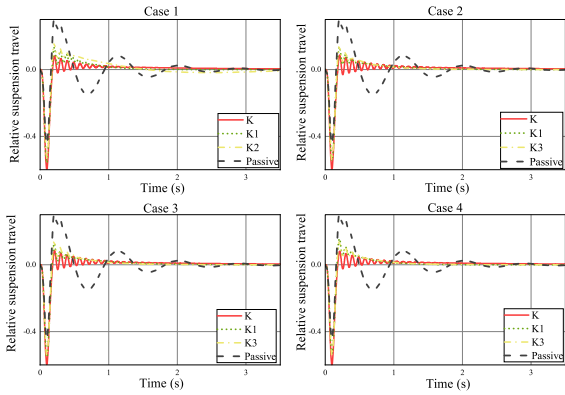


Fig. 8 Relative suspension travel under bump excitation in Case 1, Case 2, Case 3, and Case 4

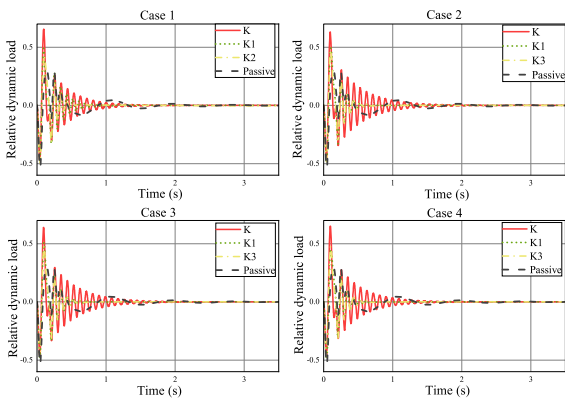


Fig. 9 Relative dynamic load under bump excitation in Case 1, Case 2, Case 3, and Case 4

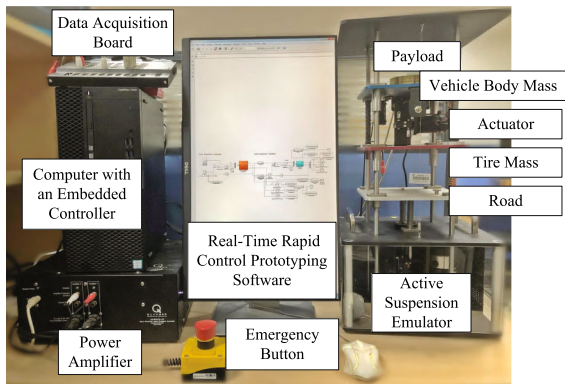


Fig. 10 Quarter-car test rig

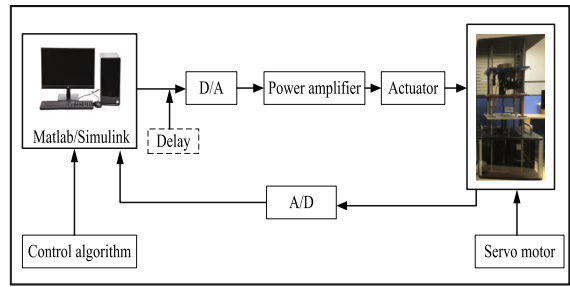


Fig. 11 Block diagram of the experimental test with quarter car test rig

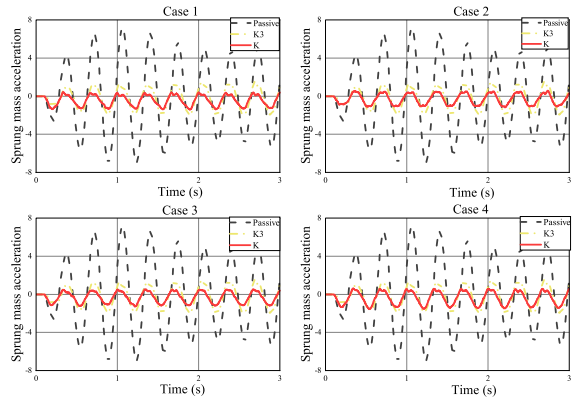


Fig. 12 Experimental sprung mass acceleration under sinusoidal bump excitation in Case 1, Case 2, Case 3, and Case 4

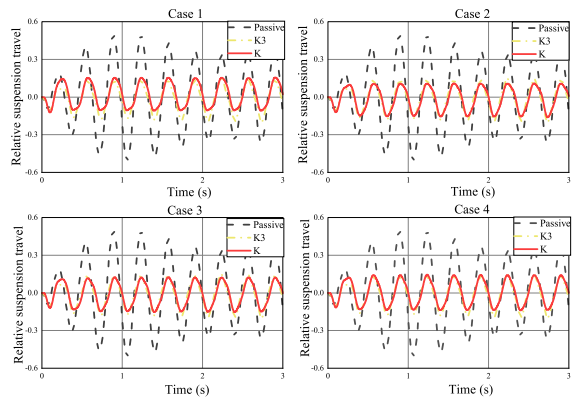


Fig. 13 Experimental relative suspension travel under sinusoidal bump excitation in Case 1, Case 2, Case 3, and Case 4

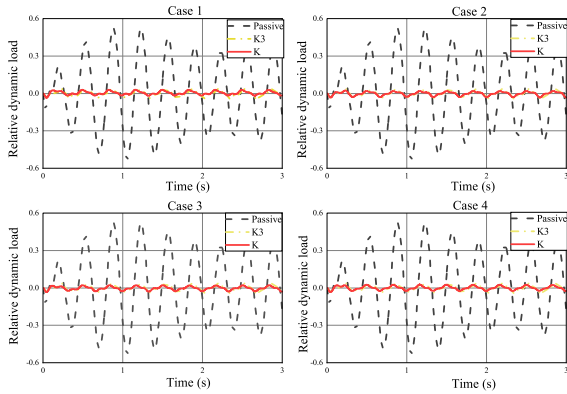


Fig. 14 Experimental relative dynamic load under sinusoidal bump excitation in Case 1, Case 2, Case 3, and Case 4

$K2$ and $K3$, which are denoted by a yellow dash-dotted line and the black scribed line describes the uncontrolled passive suspension.

Figure 4 plots the frequency response of the sprung mass acceleration in Cases 1–4. We can see that with the controller K , the acceleration values of the ASSs are lower than with the other controllers evidently. It means the proposed controller in this paper can greatly improve the ride comfort.

Figures 5 and 6 plot the relative suspension travel and dynamic load. It can be seen that controller K provides a significant improvement near the natural frequency of the sprung mass mode.

Remark 5 The main purpose of this work is to maximally improve the ride comfort of the suspension system, and at the same time meeting the mechanical constraints of the suspension dynamic travel and dynamic load. Although the Bode diagram of the relative dynamic load of the designed controller is not excellent, the main control target of this work is satisfied as well as the corresponding mechanical constraints.

4.2 Bump responses

The effectiveness of the proposed controller is verified by using a bumped road profile [36], as shown below:

$$z_r(t) = \begin{cases} \frac{A}{2} (1 - \cos(\frac{2\pi v}{l}t)), & \text{if } 0 \leq t \leq \frac{l}{v} \\ 0, & \text{if } \frac{l}{v} < t \end{cases} \quad (35)$$

where A denotes the height of the bump and l denotes the length of the bump. The parameters are set as $A =$

Table 5 Root mean square 1

Case number	Passive	K	$K1$	$K2$
Case 1	0.7616	0.1037	0.3251	0.4256
Reduced rates		86.38%	57.31%	44.11%

0.05 m and $l = 3$ m, and the forward velocity of vehicle is set as $v = 15$ m/s. The time-domain response results of Cases 1–4 are shown in Figs. 7, 8 and 9, respectively.

As shown in Fig. 7, the controller K can quickly reduce the sprung mass acceleration evidently, compared with other the controllers. It validates the effectiveness and importance of non-fragile control and stochastic method.

Figures 8 and 9 indicate that the maximum value of relative suspension travel and the maximum value of relative dynamic load are less than one, respectively. According to the conditions in (14), the ASSs satisfies the requirements of safety performance constraints.

4.3 Root mean square

Furthermore, the root mean square (RMS) values of body vertical acceleration are listed in Tables 5 and 6. As shown in Table 5, compared with the passive suspension, the RMS values of body vertical acceleration for the compared controller $K1$, $K2$ and designed controller K can be reduced by 57.31%, 44.11%, and 86.38% under Case 1, respectively. This shows that the designed controller can improve vehicle ride quality while taking time delay and safety performance constraints into account. Moreover, Table 6 shows the RMS values of body vertical acceleration under different controller parameter perturbations. This reveals that the controller parameter perturbation can cripple the performance of the ASS. Meanwhile, Table 6 also validates the effectiveness and robustness of the proposed controller.

5 Experimental results

For the sake of validating the significance and performance of the presented non-fragile H_∞ controller, experimental tests are carried out by a quarter-car test bench.

Table 6 Root mean square 2

Case number	Passive	K	$K1$	$K3$
Case 2	0.7616	0.1299	0.3399	0.3560
Reduced rates		82.94%	55.37%	53.25%
Case 3	0.7616	0.1376	0.3014	0.3560
Reduced rates		81.93%	53.98%	53.25%
Case 4	0.7616	0.1186	0.3879	0.3560
Reduced rates		84.42%	49.07%	53.25%

Table 7 Parameters of quarter car test rig

Parameter	Value	Unit	Parameter	Value
$m_s(t)$	3.45	kg	z_{max}	0.038 m
$m_u(t)$	1	kg	Δu_{max}	5 N
k_s	900	N/m	u_{max}	38.3 N
k_t	2500	N/m	φ_l	0.035 s
b_s	7.5	N s/m	φ_d	0.095 s
b_t	5	N s/m		

As shown in Fig. 10, the test rig is mainly composed of a computer with an embedded controller, a data acquisition board, an emergency button, a power amplifier, and an active suspension emulator. The active suspension emulator elements mainly contain a servo motor to push the road, a payload to simulate the vehicle load-bearing, a vehicle body mass, a tire mass, and an actuator. Figure 11 shows the block diagram of the experimental test with quarter car test rig. The parameters of this test rig are listed in Table 7. Owing to the existence of white noise and the limitations of the motor, the random road contour cannot be provided by the servo motor. Since the sine wave road profile is usually used in the experiment to interpret the performance of controllers [37], the following sine wave road profile is employed for the experiments.

$$z_r(t) = A \sin\left(\frac{2\pi v}{l} t\right) \tag{36}$$

The parameters are set as $A = 0.005$ m, $l = 5$ m, and the forward velocity of vehicle is set as $v = 36$ km/s.

Remark 6 The output feedback control of the active suspension system is implemented in Simulink numerical environment. The stochastic network-induced delay and the nonlinear factors are fully considered for solving the feedback gains. Meanwhile, a delay block is

Table 8 Control gains in experiment

Case number	K
Case 1	$[-132.20, -131.24, 2.5056]$
Case 2	$[-90.873, -114.59, 3.3945]$
Case 3	$[-109.03, -124.38, 3.4842]$
Case 4	$[-82.868, -105.05, 3.4398]$

used outside the controller to represent the network-induced delay in actuator-to-system link and an IT-2 T-S fuzzy model is introduced to describe the nonlinear characteristics of active suspension systems. In addition, road input is established in Simulink environment. The servo motor generates corresponding forces according to the road block to push the road upwards.

The local control gains of the experiment are shown in Table 8.

Moreover, the experimental comparison gains of the controllers in [17] are as follows:

$$K3 = [70.785, -29.679, -12.852, -0.5105]$$

The experimental results are shown in Figs. 12, 13 and 14. Similar to the simulation study, the controller in [17] are taken as the compared controller to demonstrate the effectiveness of the designed controller. Figures 12, 13 and 14 indicate that the designed controller is more to improve the ride comfort compared with the controllers in [17] and passive suspension.

6 Conclusions

In this research, a non-fragile IT-2 fuzzy H_∞ controller for the uncertain ASSs with the stochastic network-induced delay is presented. According to the experimental results, the designed controller was more effective to demands of driving safety, handling stability and ride comfort than the comparative cases. Moreover, some useful conclusions are summarized as follows:

- (1) The IT-2 T-S fuzzy model built in this paper fully considers the parameter uncertainties of the suspension system, and reasonably reflects the dynamic characteristics of the ASSs.
- (2) In view of a large amount of output feedback calculation and the unsatisfactory system response, the optimal output feedback control method designed in this paper not only ensures the control performance, but also reduces the computational burden.

Moreover, by introducing control gain perturbations, the control performance is further improved.

- (3) In the process of establishing Lyapunov function, the upper and lower bounds and existence of network-induced delay information are considered. The proposed approach effectively reduces the conservatism of the controller.

Future work can be considered to investigate the asynchronous constraints between the fuzzy system and the fuzzy controller. Moreover, the influencing factors of suspension frequency characteristics can be also considered in the future work.

Acknowledgements This work is supported by National Natural Science Foundation of China (Grant No. 52175127), the Natural Science Foundation of Guangdong Province of China (Grant Nos. 2022A1515011495), the China Postdoctoral Science Foundation (Grant No. 2022M712383), the Fundamental Research Funds for the Central Universities (Grant No. N2203012), the research Grant of the University of Macau (Grant No. MYRG2022-00099-FST), the Science and Technology Development Fund, Macau SAR (Grant Nos. 0018/2019/AKP and SKL-IOTSC(UM)-2021-2023), and the Guangdong Science and Technology Department (Grant Nos. 2018B030324002 and 2020B1515130001).

Funding The authors have not disclosed any funding.

Data availability The data for supporting the current study will be made available upon the reasonable request for academic use by contacting the corresponding author.

Declarations

Conflict of interest The authors declare that they have no conflict of interest.

References

- Ding, F., Han, X., Jiang, C., Liu, J., Peng, C.: Fuzzy dynamic output feedback force security control for hysteretic leaf spring hydro-suspension with servo valve opening predictive management under deception attack. *IEEE Trans. Fuzzy Syst.* **30**(9), 3736–3747 (2022)
- Zhang, Z.Y., Wang, J.B., Wu, W.G., Huang, C.X.: Semi-active control of air suspension with auxiliary chamber subject to parameter uncertainties and time-delay. *Int. J. Robust Nonlinear Control* **30**(17), 7130–7149 (2020)
- Zhao, J., Wong, P.K., Ma, X.B., Xie, Z.C.: Chassis integrated control for active suspension, active front steering and direct yaw moment systems using hierarchical strategy. *Veh. Syst. Dyn.* **55**(1), 72–103 (2017)
- Zhao, J., Wong, P.K., Li, W.F., Ghadikolaiea, M.A., Xie, Z.C.: Reliable fuzzy sampled-data control for nonlinear suspension systems against actuator faults. *IEEE ASME Trans. Mechatron.* (2022). <https://doi.org/10.1109/TMECH.2022.3184617>
- Du, Z.B., Kao, Y.G., Park, J.H.: Interval type-2 fuzzy sampled-data control of time-delay systems. *Inf. Sci.* **487**, 193–207 (2019)
- Li, H., Sun, X., Wu, L., Lam, H.K.: State and output feedback control of interval type-2 fuzzy systems with mismatched membership functions. *IEEE Trans. Fuzzy Syst.* **23**(6), 1943–1957 (2015)
- Ren, G.P., Chen, Z., Zhang, H.T., Wu, Y., Meng, H., Wu, D., Ding, H.: Design of interval type-2 fuzzy controllers for active magnetic bearing systems. *IEEE ASME Trans. Mechatron.* **25**(5), 2449–2459 (2020)
- Du, H.P., Zhang, N.: Fuzzy control for nonlinear uncertain electrohydraulic active suspensions with input constraint. *IEEE Trans. Fuzzy Syst.* **17**(2), 343–356 (2009)
- Ma, X.B., Wong, P.K., Zhao, J., Xie, Z.C.: Cornering stability control for vehicles with active front steering system using T-S fuzzy based sliding mode control strategy. *Mech. Syst. Signal Process.* **125**, 347–364 (2019)
- Rath, J.J., Defoort, M., Karimi, H.R., Veluvolu, K.C.: Output feedback active suspension control with higher order terminal sliding mode. *IEEE Trans. Ind. Electron.* **64**(2), 1392–1403 (2017)
- Song, J., Niu, Y.G., Zou, Y.Y.: A parameter-dependent sliding mode approach for finite-time bounded control of uncertain stochastic systems with randomly varying actuator faults and its application to a parallel active suspension system. *IEEE Trans. Ind. Electron.* **65**(10), 8124–8132 (2018)
- Wen, S.P., Chen, M.Z.Q., Zeng, Z.G., Yu, X.H., Huang, T.W.: Fuzzy control for uncertain vehicle active suspension systems via dynamic sliding-mode approach. *IEEE Trans. Syst. Man Cybern. Syst.* **47**(1), 24–32 (2017)
- Na, J., Huang, Y.B., Wu, X., Gao, G.B., Herrmann, G., Jiang, J.Z.: Active adaptive estimation and control for vehicle suspensions with prescribed performance. *IEEE Trans. Control Syst. Technol.* **26**(6), 2063–2077 (2018)
- Pan, H.H., Jing, X.J., Sun, W.C., Gao, H.J.: A bioinspired dynamics-based adaptive tracking control for nonlinear suspension systems. *IEEE Trans. Control Syst. Technol.* **26**(3), 903–914 (2018)
- Zheng, X.Y., Zhang, H., Yan, H.C., Yang, F.W., Wang, Z.P., Vlacic, L.: Active full-vehicle suspension control via cloud-aided adaptive backstepping approach. *IEEE Trans. Cybern.* **50**(7), 3113–3124 (2020)
- Hu, M.J., Park, J.H., Cheng, J.: Robust fuzzy delayed sampled-data control for nonlinear active suspension systems with varying vehicle load and frequency-domain constraint. *Nonlinear Dyn.* **105**(3), 2265–2281 (2021)
- Zhang, Z., Li, H., Wu, C., Zhou, Q.: Finite frequency fuzzy h control for uncertain active suspension systems with sensor failure. *IEEE/CAA J. Autom. Sin.* **5**(4), 777–786 (2018)
- Hu, C.A., Jing, H., Wang, R.R., Yan, F.J., Chadli, M.: Robust h-infinity output-feedback control for path following of autonomous ground vehicles. *Mech. Syst. Signal Process.* **70–71**, 414–427 (2016)
- Liang, D., Huang, J.: Robust output regulation of linear systems by event-triggered dynamic output feedback control. *IEEE Trans. Autom. Control* **66**(5), 2415–2422 (2021)

20. Niu, X.R., Lin, W., Gao, X.W.: Static output feedback control of a chain of integrators with input constraints using multiple saturations and delays. *Automatica* **125**, 8 (2021)
21. Shao, X.X., Naghdy, F., Du, H.P., Li, H.Y.: Output feedback h-infinity, control for active suspension of in-wheel motor driven electric vehicle with control faults and input delay. *ISA Trans.* **92**, 94–108 (2019)
22. Na, J., Huang, Y.B., Wu, X., Liu, Y.J., Li, Y.P., Li, G.: Active suspension control of quarter-car system with experimental validation. *IEEE Trans. Syst. Man Cybern.-Syst.* **52**(8), 4714–4726 (2022)
23. Han, S.Y., Zhou, J., Chen, Y.H., Zhang, Y.F., Tang, G.Y., Wang, L.: Active fault-tolerant control for discrete vehicle active suspension via reduced-order observer. *IEEE Trans. Syst. Man Cybern.-Syst.* **51**(11), 6701–6711 (2021)
24. Xiong, J., Chang, X.H., Park, J.H., Li, Z.M.: Nonfragile fault-tolerant control of suspension systems subject to input quantization and actuator fault. *Int. J. Robust Nonlinear Control* **30**(16), 6720–6743 (2020)
25. Chang, X.H., Liu, Y.: Quantized output feedback control of AFS for electric vehicles with transmission delay and data dropouts. *IEEE Trans. Intell. Transp. Syst.* **23**(9), 16026–16037 (2022)
26. Li, W.F., Xie, Z.C., Zhao, J., Wong, P.K., Li, P.S.: Fuzzy finite-frequency output feedback control for nonlinear active suspension systems with time delay and output constraints. *Mech. Syst. Signal Process.* **132**, 315–334 (2019)
27. Qi, Z., Shi, Q., Zhang, H.: Tuning of digital PID controllers using particle swarm optimization algorithm for a can-based dc motor subject to stochastic delays. *IEEE Trans. Ind. Electron.* **67**(7), 5637–5646 (2020)
28. Jin, X.J., Yin, G.D., Li, Y.J., Li, J.Q.: Stabilizing vehicle lateral dynamics with considerations of state delay of AFS for electric vehicles via robust gain-scheduling control. *Asian J. Control* **18**(1), 89–97 (2016)
29. Zhu, X.Y., Zhang, H., Wang, J.M., Fang, Z.D.: Robust lateral motion control of electric ground vehicles with random network-induced delays. *IEEE Trans. Veh. Technol.* **64**(11), 4985–4995 (2015)
30. Huang, H., Ho, D.W.C., Qu, Y.: Robust stability of stochastic delayed additive neural networks with Markovian switching. *Neural Netw.* **20**(7), 799–809 (2007)
31. Mao, X.R.: Exponential stability of stochastic delay interval systems with Markovian switching. *IEEE Trans. Autom. Control* **47**(10), 1604–1612 (2002)
32. Palhares, R.M., Peres, P.L.D.: Robust filtering with guaranteed energy-to-peak performance—an LMI approach. *Automatica* **36**(6), 851–858 (2000)
33. Wu, M., He, Y., She, J.H., Liu, G.P.: Delay-dependent criteria for robust stability of time-varying delay systems. *Automatica* **40**(8), 1435–1439 (2004)
34. Wang, G., Chen, C.Z., Yu, S.B.: Robust non-fragile finite-frequency h-infinity static output-feedback control for active suspension systems. *Mech. Syst. Signal Process.* **91**, 41–56 (2017)
35. Palacios-Quinonero, F., Rubio-Massegu, J., Rossell, J.M., Karimi, H.R.: Feasibility issues in static output-feedback controller design with application to structural vibration control. *J. Frankl. Inst. Eng. Appl. Math.* **351**(1), 139–155 (2014)
36. Zhao, J., Dong, J.G., Wong, P.K., Ma, X.G., Wang, Y.F., Lv, C.: Interval fuzzy robust non-fragile finite frequency control for active suspension of in-wheel motor driven electric vehicles with time delay. *J. Frankl. Inst. Eng. Appl. Math.* **359**(12), 5960–5990 (2022)
37. Li, W.F., Xie, Z.C., Wong, P.K., Ma, X.B., Cao, Y.C., Zhao, J.: Nonfragile h-infinity control of delayed active suspension systems in finite frequency under nonstationary running. *J. Dyn. Syst. Meas. Control Trans. ASME* **141**(6), 16 (2019)

Publisher's Note Springer Nature remains neutral with regard to jurisdictional claims in published maps and institutional affiliations.

Springer Nature or its licensor (e.g. a society or other partner) holds exclusive rights to this article under a publishing agreement with the author(s) or other rightsholder(s); author self-archiving of the accepted manuscript version of this article is solely governed by the terms of such publishing agreement and applicable law.